

EXPLICIT EQUATIONS FOR MIRROR FAMILIES TO LOG CALABI-YAU SURFACES

LAWRENCE JACK BARROTT

ABSTRACT. Mirror symmetry for del Pezzo surfaces was studied in [3] where they suggested that the mirror should take the form of a Landau-Ginzburg model with a particular type of elliptic fibration. This argument came from symplectic considerations of the derived categories involved. This problem was then considered again but from an algebro-geometric perspective by Gross, Hacking and Keel in [8]. Their construction allows one to construct a formal mirror family to a pair (S, D) where S is a smooth rational projective surface and D a certain type of Weil divisor supporting an ample or anti-ample class. In the case where the self intersection matrix for D is not negative semi-definite it was shown in [8] that this family may be lifted to an algebraic family over an affine base.

In this paper we perform this construction for all smooth del Pezzo surfaces of degree at least two and obtain explicit equations for the mirror families and present the mirror to dP_2 as a double cover of \mathbb{P}^2 .

1. Introduction

Our starting materials will be a pair (S, D) where S is a smooth del Pezzo surface of degree at least two and $D \in |-K_S|$ is a cycle of rational curves. Such pairs were first studied in [14] as relating to certain cusp singularities and were called *Looijenga pairs*. When viewed in log geometry they are *log Calabi-Yau surfaces*. Our goal will be to explicitly construct the mirror to (S, D) in a variety of cases using the Gross-Siebert program.

Mirror symmetry predicts, according to Givental's 1994 ICM lecture, that associated to a toric Fano variety V there should exist a mirror Landau-Ginzburg model (LG model). This is a pair (\check{V}, \check{W}) where \check{V} is a smooth variety and $\check{W} : \check{V} \rightarrow \mathbb{C}$ the *super-potential*, a regular function. This was extended in work of Cho and Oh, who in [6] realised that a choice of effective anti-canonical divisor played a role in determining the LG model.

Received February 1, 2019; Revised May 17, 2019; Accepted November 6, 2019.

2010 *Mathematics Subject Classification*. 14J33, 14N10, 14T05.

Key words and phrases. Mirror symmetry, Gross-Siebert, Fano surfaces, scattering diagrams.

The paper [8] constructs a formal smoothing of the n -vertex, a cycle of planes meeting along their axes, over $\text{Spec } k[[NE(S)]]$. The key result for us of [8] is the following.

Theorem 1.1. *Let (S, D) be a pair as above and suppose that the self intersection matrix of D is not negative semi-definite. Then the above formal smoothing lifts to an algebraic family over the entirety of $\text{Spec } k[[NE(S)]]$.*

Proof. This is Theorem 0.2 of [8]. □

This paper shows that the equations can be calculated algorithmically from a scattering diagram on an associated fan. We apply this to prove our main theorem:

Theorem 1.2. *Let S be a degree two del Pezzo surface and $D \in |-K_S|$ a cycle of rational curves. Then the mirror LG model is a double cover of \mathbb{A}^2 branching over a quartic curve. The coefficients of the defining equation are described by the birational geometry of S .*

We also provide algebraic descriptions of the higher degree surfaces. See forthcoming work by Gross, Hacking and Keel for a fully detailed account of the mirror LG model to dP_3 .

Acknowledgements. This work was an initial project in my PhD thesis, as suggested by Mark Gross. It was from him that I learnt much of the background and motivation for the Gross-Siebert program. Various discussions about the material of [8] with Tyler Kelly, Zhi Jin, Ben Morely and Andrea Petracci proved immensely helpful to my understanding of the material. This project was included in my thesis and I must thank Tom Coates and Pelham Wilson for examining me, and ironing out various parts of the exposition and of course Mark Gross who helped to review the initial draft of this paper and suggesting the problem.

This project was funded by a variety of sources: by an Internal Graduate Studentship provided by Trinity College, by a research studentship provided by the Cambridge Philosophical Society and by Final Term Funding provided by the Department for Pure Mathematics and Mathematical Statistic (DPMMS) in Cambridge and a research assistantship at NCTS in Taipei.

2. Constructions of mirror families to del Pezzo surfaces

Throughout this paper let S be a smooth complex del Pezzo surface and $D = D_1 \cup D_2 \cup \dots \cup D_n$ an anti-canonical cycle of rational curves with n at least three (we will explain separately how to deal with the case of dP_2). Recall that by the classification of del Pezzo surfaces this ensures that S is isomorphic to one of the following:

- $\mathbb{P}^1 \times \mathbb{P}^1$.
- The blow-up of \mathbb{P}^2 in zero through eight points in general position.

The respective Chow groups $A_1(S)$ are generated by

- The pullback of a point under the two projection maps.
- A hyperplane class H and the exceptional curves E_1, \dots, E_{9-d} ,

whilst the groups $A_0(S)$ and $A_2(S)$ are isomorphic to \mathbb{Z} generated by a point and a fundamental class respectively.

This pair can be thought of in many ways, but perhaps the most appealing to those studying mirror symmetry is as a *log Calabi-Yau varieties*, varieties such that there is a non-vanishing differential form on $S \setminus D$ with at worst logarithmic singularities along D . Of these the surfaces $\mathbb{P}^1 \times \mathbb{P}^1$, \mathbb{P}^2 , dP_8 , dP_7 and dP_6 are all toric and mirror families can be constructed using the techniques of [6]. The next three surfaces were studied in [3]. We will show that the prediction there agrees with the algebraic construction of [8]. We will then handle one of the remaining two cases, the blow up in seven points. Precisely the same techniques can be applied in the case of dP_1 but due to the computational limitations we do not pursue this.

In the toric case the base is a fan for the variety in the sense of [7]. The base of the SYZ fibration for a toric del Pezzo surface is just the fan. This can be recovered, up to a choice of embedding into \mathbb{R}^2 , as the dual intersection complex of D .

Construction 2.1. Let $D = D_1 \cup D_2 \cup \dots \cup D_n$ be a cycle of rational curves on a smooth surface S such that $D_i \cap D_j$ is a single point just when i and j differ by 1 mod n and otherwise is empty (in the case $n = 2$ we relax this to saying that there are two points in the unique intersection $D_1 \cap D_2$). Then $\Delta_{(S,D)}$ contains precisely one zero-dimensional cell $\{0\}$ corresponding to the interior $S \setminus D$. For each component D_i , $\Delta_{(S,D)}$ contains a one-dimensional cone with v_i its primitive generator. Attach the zero-dimensional cone as 0 inside each of these rays. Now introduce a two-dimensional cone in $\Delta_{(S,D)}$ for each intersection point of $D_i \cap D_j$, spanned by v_i and v_j . This produces the *dual intersection complex* $\Delta_{(S,D)}$ as a cone complex but it carries more structure. We write B to be the underlying topological space of the cone complex $\Delta_{(S,D)}$. It is homeomorphic to \mathbb{R}^2 . We give $B \setminus \{0\}$ an affine manifold structure by defining an affine coordinate chart by embedding the union of the cones $\mathbb{R}^{\geq 0}v_{i+1} \oplus \mathbb{R}^{\geq 0}v_i$ and $\mathbb{R}^{\geq 0}v_i \oplus \mathbb{R}^{\geq 0}v_{i-1}$ into \mathbb{R}^2 via the relations $v_{i-1} \mapsto (1, 0)$, $v_i \mapsto (0, 1)$ and $v_{i+1} \mapsto (-1, -D_i^2)$. This expresses $\Delta_{(S,D)}$ not just as a complex of sets but an affine manifold with singularities (indeed a single singularity at the origin).

This construction makes perfect sense outside of the toric case only it may not embed via an affine map into \mathbb{R}^2 . This fits into the general picture that the base of the SYZ fibration should be an affine manifold with singularities, a topological manifold with charts away from codimension two such that the transition functions lie in the affine transformation group $\mathbb{R}^n \rtimes Sl(\mathbb{Z}^n)$. That the dual intersection complex does embed into \mathbb{R}^2 in the toric case is a consequence of the following lemma:

Lemma 2.2 (Toric reconstruction). *Let S be a compact toric surface and D the toric boundary. Then (S, D) is a Looijenga pair, $\Delta_{(S, D)}$ embeds into \mathbb{R}^2 and any choice of embedding gives the fan for a toric variety isomorphic to S .*

Proof. See [7, Chapter 3]. \square

An integral affine manifold M carries a sheaf of integral vector fields, which we write Λ_M . On a chart this is isomorphic to the constant sheaf with coefficients \mathbb{Z}^n . The transition functions naturally give identifications of these constant sheaves. We define $M(\mathbb{Z})$ to be the set of points of M with integer coordinates in some, hence all, integral affine coordinate chart.

Given a choice of ample divisor H on S toric, the fan $\Delta_{(S, D)}$ carries a natural choice of piecewise linear function up to a choice of global linear function and we denote this ϕ . Such a function is defined by how it changes where it is non-linear. If $\phi_{v_i, v_{i+1}}$ denotes the linear extension of ϕ restricted to $\mathbb{R}^{\geq 0}v_i + \mathbb{R}^{\geq 0}v_{i+1}$, then we determine ϕ by insisting that $\phi_{v_i, v_{i+1}} - \phi_{v_{i-1}, v_i} = (H \cdot D_i)n_i$, where n_i is a primitive element of the dual space vanishing on v_i and positive on $v_i\mathbb{R}^{\geq 0} + v_{i+1}\mathbb{R}^{\geq 0}$.

In the toric case the ring of ϑ functions is very simple, for each point P in $M(\mathbb{Z})$ introduce a formal element ϑ_P . The product of ϑ_P and ϑ_Q is then defined to be

$$(2.1) \quad \vartheta_P \vartheta_Q = z^{\phi(P+Q) - \phi(P) - \phi(Q)} \vartheta_{P+Q}.$$

Let us calculate the mirror in one of the toric cases, \mathbb{P}^2 . As we said in the introduction that in the toric case there are no corrections from singularities of the fibration.

Example 2.3. Our first goal is to find the fan. Fortunately we learnt a fan for \mathbb{P}^2 back in infancy: it has one cells generated by $(1, 0)$, $(0, 1)$ and $(-1, -1)$ as shown in Figure 2.1.

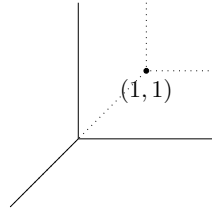


FIGURE 2.1

Calculating the product defined above, using the ample divisor H a class of a line in \mathbb{P}^2 , one finds $\vartheta_{(1,0)}\vartheta_{(0,1)} = z\vartheta_{(-1,-1)}$. As in the basis constructions of [5] these functions morally ought to produce an embedding of the mirror into affine space and their sum should be the super-potential. Doing this we obtain the mirror as being \mathbb{G}_m^2 with superpotential $x + y + z/xy$. As expected this is the mirror predicted by other constructions.

Gross and Siebert were influenced initially by the Mumford degeneration and we turn to this for guidance on how to construct a choice of ϕ in the non-toric case. This construction will also show how different choices of ample H can give rise to different mirrors.

We fix the data of all the Looijenga pairs (S, D) we will study, so let us record here a choice of boundary divisor and affine manifold for all the non-toric del Pezzo surfaces. Here we record the boundary divisor in \mathbb{P}^2 before blowing up. The circles represent points to be blown up, with the exceptional divisor included in the boundary if the circle is red. Since we can't embed the dual complex as an affine manifold in \mathbb{R}^2 , we instead provide a list of cones in \mathbb{R}^2 and an integral affine isomorphism between two of these cones. The dual intersection complex is then obtained by identifying these two cones using this isomorphism. In the pictures below the cone shaded grey is identified integral linearly with the standard first quadrant, whilst the dotted region is removed entirely.

Surface	Boundary	Class of boundary	Dual complex
dP_5		$\cup D_i = E_1 \cup (H - E_1 - E_2) \cup E_2 \cup (H - E_2 - E_3) \cup (H - E_1 - E_4)$	
dP_4		$\cup D_i = E_1 \cup (H - E_1 - E_2) \cup (H - E_3 - E_4) \cup (H - E_1 - E_5)$	
dP_3		$\cup D_i = (H - E_1 - E_2) \cup (H - E_3 - E_4) \cup (H - E_5 - E_6)$	
dP_2		$\cup D_i = (H - E_1 - E_2) \cup (2H - E_3 - E_4 - E_5 - E_6 - E_7)$	

2.1. The Mumford degeneration

The construction of the mirror family was inspired by the Mumford degeneration of an Abelian variety to the union of toric varieties. Let us recall the construction of [16].

Example 2.4. Let $N \cong \mathbb{N}^k$ be a lattice, $B \subset N_{\otimes \mathbb{N}} \mathbb{R}$ be a lattice polyhedron, \mathcal{P} a lattice polyhedral decomposition of B and $\phi : B \rightarrow \mathbb{R}$ a strictly convex piecewise linear integral function. One takes the graph over ϕ to produce a

new polyhedron

$$\Gamma(B, \phi) := \{(n, r) \in N_{\mathbb{R}} \oplus \mathbb{R} \mid n \in B, r \geq \phi(n)\}.$$

This produces a lattice polyhedron unbounded in the positive direction on \mathbb{R} . To construct a family from this we perform a cone construction, let $C(\Gamma)$ be the closure of the cone over $\Gamma(B, \phi)$:

$$C(\Gamma) = \overline{\{(n, r_1, r_2) \in N_{\mathbb{R}} \oplus \mathbb{R} \oplus \mathbb{R} \mid (n, r_1) \in r_2 \Gamma(B, \phi)\}}.$$

This carries an action of \mathbb{R}^+ given by translating the second component of $\Gamma(B, \phi)$. The integral points of $C(\Gamma)$ form a graded monoid and we can take *Proj* of this to produce a variety projective over \mathbb{A}^1 . We write this $\mathbb{P}_{\Gamma(B, \phi)}$. The general fibre is a toric variety, whilst the fibre over the origin is a union of toric varieties.

The construction of [8] mimics this in reverse: it claims that the central fibre should be the n -vertex, which for $n > 2$ is a cycle of n copies of \mathbb{A}^2 glued adjacently along their axes, and then attempts to smooth. We cannot hope to have global coordinates as in the toric Mumford degeneration, only local coordinates. To incorporate this data the authors of [8] define a twist of the tangent sheaf which has enough global sections, in particular the function ϕ lifts to a section of this bundle.

Definition 2.5. Let (S, D) be a Looijenga pair with associated dual intersection complex $\Delta_{(S, D)}$ and let $\eta : NE(S) \rightarrow M$ be a homomorphism of monoids. We want to construct a multi-valued piecewise linear function on $\Delta_{(S, D)}$ which will bend only along the one-cells. This will be a collection of piecewise linear functions defined on open subsets of B which differ by linear functions on overlaps. Such functions are determined by their bends at one-cells, which are encoded as follows. For a one-cell $\tau = \mathbb{R}^{\geq 0}v_i$, choose an orientation σ_+ and σ_- of the two two-cells separated by τ and let n_τ be the unique primitive linear function positive on σ_+ and annihilating τ . We want to construct a representative ϕ_i for ϕ on $\sigma_+ \cup \sigma_-$. Writing ϕ_+ and ϕ_- for the linear function defined by ϕ_i on σ_+ and σ_- , the function ϕ_i is then defined up to a linear function by the requirement that

$$\phi_+ - \phi_- = n_\tau \otimes \eta([D_i]).$$

Such a function is convex in the sense of [8] Definition 1.11, and one says that it is *strictly convex* if $\eta([D_i])$ is not invertible for any i .

This function determines a $M^{gp} \otimes \mathbb{R}$ -torsor \mathbb{P} as defined in [12], Construction 1.14, on $B \setminus \{0\}$ which is trivial on each $(\sigma_+ \cup \sigma_-) \setminus \{0\}$, i.e., is given by $((\sigma_+ \cup \sigma_-) \setminus \{0\}) \times (M^{gp} \otimes \mathbb{R})$. These trivial torsors are glued on the overlap of two adjacent such sets, namely on $\mathbb{R}^{\geq 0}v_i \oplus \mathbb{R}^{\geq 0}v_{i+1}$, via the map

$$(x, p) \mapsto (x, p + \phi_{i+1}(x) - \phi_i(x))$$

which induce isomorphisms on the monoid of points lying above ϕ . This construction is designed to allow us to run the Mumford construction locally, even

if we cannot run it globally. Let $\pi : \mathbb{P} \rightarrow B \setminus \{0\}$ be the projection map, and we write \mathcal{M} for the sheaf $\pi_*(\Lambda_{\mathbb{P}})$, bearing in mind that \mathbb{P} also has the structure of an affine manifold. Then there is a canonical exact sequence

$$0 \rightarrow \underline{M}^{gp} \rightarrow \mathcal{M} \xrightarrow{r} \Lambda_B \rightarrow 0.$$

We write r for the second map in this sequence. This will not be mentioned again until we define the canonical scattering diagram so keep this in mind until then. Furthermore, [10], Definition 1.16 gives a subsheaf of monoids $\mathcal{M}^+ \subset \mathcal{M}$.

If one performs this construction in the case of a toric variety with the function ϕ and pairs it with an ample class one obtains the height function we used in the Mumford degeneration. From this Gross, Hacking and Keel use such a ϕ to produce a canonical deformation of the n -vertex corresponding to the case where there are no corrections. We introduce the corrected version directly.

3. Scattering diagrams

In Mumford’s degeneration of an Abelian variety above all the fibres of the SYZ fibration on a generic member of the family are smooth. This cannot be the case for a special Lagrangian fibration of a general variety, there must be some singular fibres in the interior and around these singular fibres there will be some monodromy action. This monodromy is an obstruction to the naive toric product rule on the ϑ being well defined on the mirror. Thus one needs a corrected notion of this product, which from symplectic geometry can be done by counting so-called Maslov index two disks as described in [2]. These can be generated by gluing on Maslov index zero disks onto standard Maslov index two disks. Rather than trying to make this symplectic heuristic precise, we instead are motivated by this picture as follows. If we stand well away from the singularities and tropicalise these Maslov index zero disks they appear to be a collection of lines passing out from the origin together with the information of their class. This data is the inspiration for the definition below of a scattering diagram on the base B .

Definition 3.1. Let B be an affine manifold with a single singularity, with B homeomorphic to \mathbb{R}^2 with singularity at the origin, so that $B^* := B \setminus \{0\}$ is an affine manifold. Let \mathcal{M} be a locally constant sheaf of Abelian groups on B^* with a subsheaf of monoids $\mathcal{M}^+ \subset \mathcal{M}$ and equipped with a map $r : \mathcal{M} \rightarrow \Lambda_B$. Let \mathcal{J} be a sheaf of ideals in \mathcal{M}^+ with stalk \mathcal{J}_x maximal in \mathcal{M}_x^+ for all $x \in B^*$. Let \mathcal{R} denote the sheaf of rings locally given by the completion of $k[\mathcal{M}^+]$ at \mathcal{J} . A *scattering diagram with values in the pair $(\mathcal{M}, \mathcal{J})$ on B* is a function f which assigns to each rational ray from the origin an section of the restriction of \mathcal{R} to the ray. We require the following properties of this function:

- For each \mathfrak{d} one has $f(\mathfrak{d}) = 1 \pmod{\mathcal{J}|_{\mathfrak{d}}}$.
- For each n there are only finitely many \mathfrak{d} for which $f(\mathfrak{d})$ is not congruent to $1 \pmod{\mathcal{J}|_{\mathfrak{d}}^n}$. These \mathfrak{d} are called *walls*.

- For each ray \mathfrak{d} and for each monomial z^p appearing in $f(\mathfrak{d})$ one has $r(p)$ tangent to \mathfrak{d} . A line for which $r(p)$ is a positive generator of \mathfrak{d} for all p with $c_p \neq 0$ is called an *incoming ray*. If instead $r(p)$ is a negative generator of \mathfrak{d} for all p with $c_p \neq 0$, it is called an *outgoing ray*.

We denote such an object by the tuple $(B, f, \mathcal{M}, \mathcal{J})$. We say that $(B, f, \mathcal{M}, \mathcal{J})$ is obtained from $(B, f', \mathcal{M}, \mathcal{J})$ by *adding outgoing rays* if for each ray \mathfrak{d} one can write $f(\mathfrak{d}) = f'(\mathfrak{d})(1 + \sum(c_p z^p))$ where for each monoid element p with $c_p \neq 0$ the vector $-r(p)$ is a generator of \mathfrak{d} .

In our case the sheaf of monoids \mathcal{M}^+ will be as given in Definition 2.5, with the monoid M being a finitely generated sharp submonoid of $H_2(S, \mathbb{Z})$ containing $NE(S)$, the monoid generated by effective curves on S . Being sharp means the only invertible element of M is the identity element, and so the maximal ideal is just the complement of the identity. We introduce the choice of scattering diagram, the *canonical scattering diagram*, and then motivate and define each term appearing. A ray $\mathfrak{d} = (av_i + bv_{i+1})\mathbb{R}^{\geq 0}$ specifies a blow up of S given by refining the fan until \mathfrak{d} is a one-cell and all the two-cells are integrally isomorphic to $(\mathbb{R}^{\geq 0})^2$. The ray \mathfrak{d} then corresponds to a component C in the inverse image of D . To this ray then we assign the power series

$$f(\mathfrak{d}) := \exp \left[\sum_{\beta} k_{\beta} N_{\beta} z^{\eta(\pi_*(\beta)) - k_{\beta} m'_{\mathfrak{d}}} \right],$$

where $m'_{\mathfrak{d}}$ is the unique lift of a primitive outward pointing tangent vector $m_{\mathfrak{d}}$ to \mathfrak{d} not contained in the relative interior of $\mathcal{M}|_{\mathfrak{d}}$. The number N_{β} counts the number of relative curves mapping to (S, D) tangent to C to maximal order k_{β} at a single point as outlined in [8] at the beginning of Section 3. This construction may also be run using logarithmic Gromov-Witten invariants rather than these blow ups, see [11] for the definition, and this will be explored in future work of Gross and Siebert.

Conjecturally this encodes the glueing data for a generating set of the open Gromov-Witten invariants. It should be possible to recreate the entire Gromov-Witten theory of S , both open and closed from this data but this problem is very difficult.

3.1. Broken lines

To encode the Maslov index two disks themselves we collapse them onto a skeleton in the base of the SYZ fibration, having pushed all the singularities to the origin. Then following [15] the disks appear as balanced tropical curves together with a mark of the class that they lie in. The skeleta of these disks are trivalent graphs with one leg ending at the origin and the other two legs passing to infinity. The definition below defines how one of these legs behave, the full picture only arising once we have discussed pairs of pants and even then we suppress the third leg which by necessity ends at origin.

Definition 3.2. A *broken line* from $v \in B(\mathbb{Z})$ to $P \in B$ on a scattering diagram (B, f, R, J) is a choice of piecewise linear function $l : \mathbb{R}^{\leq 0} \rightarrow B$ and a map $m : \mathbb{R}^{\leq 0} \rightarrow \prod_{t \in \mathbb{R}^{\leq 0}} \mathcal{R}_{l(t)}$ such that the following hold:

- l has only finitely many points where it is non-linear and these only occur where l maps into a rational ray of B .
- $l(0) = P$.
- $l(t)$ lies in the same cone as v and is parallel to v for all t sufficiently negative.
- l does not map an interval to a ray through the origin.
- $m(t) \in \mathcal{R}_{l(t)}$ for all t and is a monomial in this ring, written as $c_t z^{m_t}$. Further, on each domain of linearity of l , $m(t)$ is given by a section of \mathcal{R} pulled back to this domain of linearity.
- For t very negative, $m_t \in \mathcal{M}_{l(t)}^+$ is the unique element not lying in the interior of this monoid satisfying $r(m_t) = v$.
- $r(m(t_0)) = -\frac{\partial l}{\partial t} \Big|_{t=t_0}$ wherever l is linear.
- m only changes at those points where l is non-linear.
- Let $t \in \mathbb{R}^{\leq 0}$ be a point where l is non-linear. We write $\partial(l_+)$, $\partial(l_-)$, m_+ and m_- for the values of $\partial l / \partial t$ and m on either side of t . Suppose that $l(t)$ lies on a ray \mathfrak{d} with primitive normal vector $n_{\mathfrak{d}}$, negative on $\partial(l_-)$. Then m_+ is a monomial term of $m_- f_{\mathfrak{d}}^{\langle n_{\mathfrak{d}}, \partial(l_-) \rangle}$.

There is more technical content in [8] exploring how to deform the Mumford construction to produce a formal smoothing of the n -vertex. We do not concern ourselves with those results at the moment since we now have enough to define the multiplication rule on the ϑ -functions. In [10] Gross, Hacking and Siebert introduce an entirely abstract construction of the ϑ -functions.

The key data we will need is the count of pairs of pants, which are expressed in terms of broken lines as pairs of broken lines (l_P, m_P) and (l_Q, m_Q) from P and Q respectively to an irrational point near to R such that $(\partial l_P / \partial t)|_{t=0} + (\partial l_Q / \partial t)|_{t=0} = R$. Let $T_{P,Q \rightarrow R}$ denote the set of such pairs.

We have seen on page 142 how to define a product on the ϑ -functions in the toric case, so let us now study the general case. The outcome of our conversation about Hochschild cohomology was that the ring of regular functions on the mirror is the degree zero part of symplectic cohomology of the original variety.

To define the ring of ϑ functions we follow [9] and for each integral point P in B introduce a symbol ϑ_P . As a k -vector space the ring $QH(\tilde{W})$ is freely generated by the ϑ_P . We take the content of [8] Theorem 2.34 as the definition of the product of ϑ_P and ϑ_Q , so the product $\vartheta_P \vartheta_Q$ is equal to

$$\sum_R \sum_{((l_P, m_P), (l_Q, m_Q)) \in T_{P,Q \rightarrow R}} m_P(0) m_Q(0) \vartheta_R.$$

This is analogous to the approach of [10]. A key result of [8] is that for fixed order J^n and for a consistent scattering diagram in the sense of [8], Definition

2.26, this does not depend on the choice of irrational point near R . This consistency property will hold in particular for the canonical scattering diagrams considered below. This sum need not terminate and indeed will in general only produce a power series. However, in the case that D supports an ample divisor, this power series will in fact be a polynomial. Our goal in what follows is to limit the terms which can occur and describe a generating basis of the ϑ -functions.

3.2. The combinatorics of scattering diagrams

We now explain how to use these functions to embed the mirror into affine space. At the moment it is not clear that the relations between the ϑ functions should be algebraic. Let us explain how to exploit the structure of a scattering diagram to prove algebraic convergence. To do this we require an example to work with, for simplicity the del Pezzo surface dP_5 .

Example 3.3. Figure 3.1 below gives a choice of boundary divisor, where circles denote blown-up points and red lines denote components of D . From

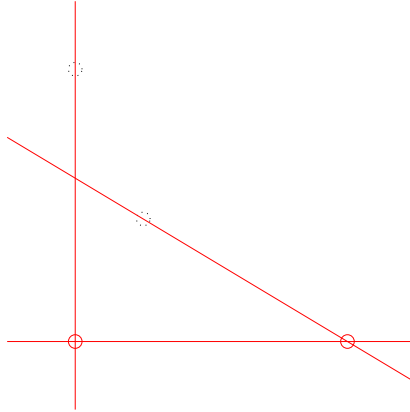


FIGURE 3.1

this we construct the base of the scattering diagram as in Figure 3.2, where the grey section is glued isomorphically to the standard upper right quadrant

In this case one can construct the entire scattering diagram: it is finite and only non-trivial on the one-cells. We will not do this since in future examples the scattering diagram will be non-trivial on a dense set of rays.

Each point of B defines a curve class as via $a v_i + b v_{i+1} \mapsto aD_i + bD_{i+1}$. Define the piecewise linear function E on B given by $-K_S \cdot (aD_i + bD_{i+1})$. From the Fano condition this defines a strictly convex piecewise linear function on the space B which is positive everywhere but at the origin. The function E extends to a linear function on the tangent space at each point in the interior

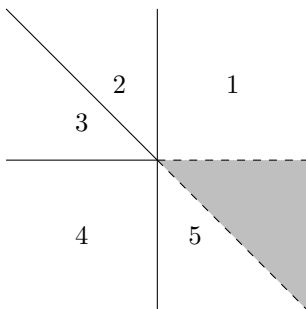


FIGURE 3.2

of a maximal cell. This allows us to evaluate E on tangent vectors to broken lines away from one-cells.

In fact, given a broken line, $E(\partial l/\partial t)$ is increasing as a function of t . Indeed, at a point t where l is non-linear by definition the tangent vector changes by a positive generator of the ray \mathfrak{d} , and E is positive on this generator. Similarly if l crosses from one maximal cell of B to another then by convexity of E the value of $E(\partial l/\partial t)$ increases.

We use this as follows. Suppose that two broken lines (l_1, m_1) and (l_2, m_2) from v_1 and v_2 combine to form a pair of pants at P . Then by definition we must have

$$(\partial l_1/\partial t)|_{t=0} + (\partial l_2/\partial t)|_{t=0} + P = 0.$$

Since $E(P) \geq 0$, and $-E(v_i) \leq E((\partial l_i/\partial t)|_{t=0})$, we see that $E(v_1)$ and $E(v_2)$ control how many new maximal cells l_1 and l_2 can enter, and how many times they can bend.

Let us begin by understanding what could possibly contribute to the product $\vartheta_{(-1,0)}\vartheta_{(0,1)}$. Let us number the two-cells anti-clockwise starting at the upper right cell as in Figure 3.2.

Let l_1 be a broken line coming from $(-1, 0)$ and l_2 a broken line from $(0, 1)$. We have that $E((-1, 0)) = E((0, 1)) = 1$. This immediately implies that $0 \leq E(P) \leq 2$. Further, if $E(P) = 2 - n$, then the total number of bends and crossings of one-dimensional cells of l_1 and l_2 is n . First note that $n = 0$ does not occur: since v_1 and v_2 are in different cones, at least one of the broken lines must cross a one-cell. If $n = 1$, then we cross one one-cell and further bends or crossings can occur. There is then only one possibility, the obvious pair of pants as described in Figure 3.3a contributing to $\vartheta_{(-1,1)}$. Finally let us study the case $n = 2$. In this case, $E(P) = 0$, hence $P = 0$, and we can choose a point near the origin, say in the second two-cell. If l_2 enters the grey region as detailed in Figure 3.3c it emerges moving in the direction $(-1, 0)$ and so has $E(\partial l/\partial t) = 1$. Therefore in order to reach the second cell, it must cross two more one-cells, and hence it can't contribute to a pair of pants. Thus l_2 must start in cell 2 and never leaves it.

A similar argument shows that l_1 can only pass from cell 3 to cell 2, and either l_1 or l_2 bends at a ray $\mathbb{R}^{\geq 0}v$ with $E(v) = 1$ and $v \in B(\mathbb{Z})$. There is only one choice for such a ray, namely the one-cell separating cells 2 and 3. See Figure 3.3b.

In general, there will only be a finite number of rays with bounded E and only a finite combination of bends. Thus in more complicated cases this analysis can be implemented in a computer algebra package via the algorithm outlined in Algorithm 1 and a non-optimised version written in Python is available from me on request.

Algorithm 1 Theta relations algorithm

```

1: object AFFINEMANIFOLD
  ▷ Define a data structure consisting of a fan  $\Sigma$ , a piecewise linear function  $\phi$  and a collection of integer points of  $\Sigma$ ,  $\Sigma_{\mathbb{Z}}$ .
2: object BROKENLINE
  ▷ Define a data structure consisting of an initial direction  $v$ , a monomial, a tangent direction thought of as  $\partial l / \partial t |_{t=0}$  and a list of points  $P_i$  generating rays along which the broken line bent
3: function PRODUCTFORMULA( $l_1, l_2$ , affinemanifold)
  ▷ Define a function of two broken lines with tangent directions  $v_1$  and  $v_2$  in an affine manifold, affinemanifold which finds all possible terms appearing in the product  $\vartheta_{v_1} \vartheta_{v_2}$ 
4:   int maxE :=  $\phi(v_1) + \phi(v_2)$ 
5:   def endpoints := The set of points in  $\Sigma_{\mathbb{Z}}$  such that  $\phi(P) \leq \max E$ .
6:   for P in endpoints do
7:     if  $l_1$  and  $l_2$  could pass through P and  $v_1 + v_2 + P = 0$  then
8:       print the data of how  $l_1$  and  $l_2$  have bent
9:     if  $l_1$  could pass through P then
10:      def newline :=  $l_1$  but now also scattering off of  $\mathbb{R}^{\geq 0}P$  as well
11:      ProductFormula (newline,  $l_2$ )
12:     if  $l_2$  could pass through P then
13:      def newline :=  $l_2$  but now also scattering off of  $\mathbb{R}^{\geq 0}P$  as well
14:      ProductFormula ( $l_1$ , newline)
15: def affinemanifold := AffineManifold( ... )
  ▷ Define the base of the appropriate scattering diagram
16: def  $L_1$  := BrokenLine ( ... )
  ▷ Define  $L_1$  to be a broken line, not scattering off of any rays with initial direction  $v_1$ 
17: def  $L_2$  := BrokenLine ( ... )
  ▷ Define  $L_2$  to be a broken line, not scattering off of any rays with initial direction  $v_2$ 
18: ProductFormula ( $L_1, L_2$ , affinemanifold)

```

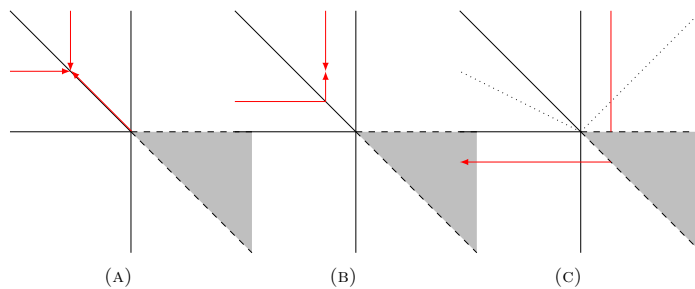


FIGURE 3.3

Doing this systematically for each pair $\vartheta_{v_{i-1}}\vartheta_{v_{i+1}}$ we can find schematic relations for the products which highlight which relative invariants we need to find. Filling out the relations for dP_5 we find the following relations.

$$(3.1) \quad \vartheta_{(1,0)}\vartheta_{(-1,1)} = g_1\vartheta_{(0,1)} + f_1,$$

$$(3.2) \quad \vartheta_{(0,1)}\vartheta_{(-1,0)} = g_2\vartheta_{(-1,1)} + f_2,$$

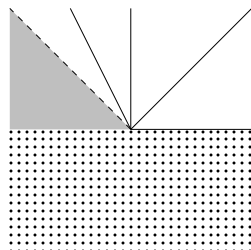
$$(3.3) \quad \vartheta_{(-1,1)}\vartheta_{(0,-1)} = g_3\vartheta_{(-1,0)} + f_3,$$

$$(3.4) \quad \vartheta_{(-1,0)}\vartheta_{(1,0)} = g_4\vartheta_{(0,-1)} + f_4,$$

$$(3.5) \quad \vartheta_{(0,-1)}\vartheta_{(0,1)} = g_5\vartheta_{(1,0)} + f_5.$$

The terms f_i count curves meeting D_i at a single point with tangency order one together with some monomials coming from broken lines looping around the origin.

As in the work of Hulya Arguz [1] the easy case is when the boundary consists of at least four components and the corresponding algebra is a quadratic algebra. The three component case is tractable but to compute the two component case dP_2 it is best to blow up the two intersection points of the two divisors. This refines the dual complex but keeps the interior $S \setminus D$ invariant. As a consequence, this changes the mirror family because the base $\text{Spec } k[P]$ increases in dimension. However, the mirror family to the original surface can be found by restricting to a subfamily, see [8], Section 6.2 for details. In keeping with our previous notation we denote the exceptional curves over these by E_8 and E_9 . The choice of dual complex now becomes:



we re-label the theta functions by the corresponding cohomology class, so ϑ_{D_i} for ϑ_i , further we write ϑ_{nD_i} for the function ϑ_{nv_i} . With these labels we can apply the techniques of Example 3.3 to show that the possible terms appearing in the relations between the theta functions become:

$$(3.6) \quad \vartheta_C \vartheta_L = r_1 \vartheta_{E_8} + r_2 \vartheta_{E_9} + r_3 + c_1(E_8),$$

$$(3.7) \quad \begin{aligned} \vartheta_{E_8} \vartheta_{E_9} &= r_4 \vartheta_{3L} + \vartheta_{2L} c_1(L) + \vartheta_L c_2(L) + c_3(C) + r_5 \\ &+ \vartheta_C c_2(C) + \vartheta_{2C} c_1(C) + r_6 \vartheta_{3C}, \end{aligned}$$

$$(3.8) \quad \vartheta_C^3 = \vartheta_{3C} + c_1(L) \vartheta_C + r_7 + c_1(E_9) + r_8 + r_9 \vartheta_{E_8} + r_{10} \vartheta_{E_9},$$

$$(3.9) \quad \vartheta_L^3 = \vartheta_{3L} + c_1(C) \vartheta_L + r_{11} + c_1(E_8) + r_{12} + r_{13} \vartheta_{E_9} + r_{14} \vartheta_{E_8},$$

$$(3.10) \quad \vartheta_C^2 = \vartheta_{2C} + r_{15} \vartheta_C + c_1(L),$$

$$(3.11) \quad \vartheta_L^2 = \vartheta_{2L} + r_{16} \vartheta_L + c_1(C),$$

where the functions r_i come from the combinatorics of broken lines which don't bend. The monomials which they carry come from the fact that the values of $\phi(\partial l / \partial t)$ are different at the start and end of the broken lines. The functions $c_n(D)$ are counts of broken lines bending due to curves tangent to a class D at a single point to order n . It is this finite list of open Gromov-Witten invariants which we must calculate. To calculate these invariants we have two options, either one could directly compute the moduli space and find the degree of the virtual fundamental class or one can use properties of the scattering diagram. Since we have not yet explained the role monodromy plays in the scattering diagram we will do the latter since it forms an important tool in the theory.

4. Explicit Gromov-Witten counts and monodromy

We cannot apply the Mumford construction globally in the non-toric case since the function ϕ is not global but we can apply it locally to each face. To do so if τ is a one- or two-dimensional face of $\Delta_{(S,D)}$, we write $\Delta_{(S,D)}/\tau$ for the localised fan at τ , i.e., the fan given by adding $\mathbb{R}\tau$ to each cone containing τ and removing cones of $\Delta_{(S,D)}$ not containing τ . Then after choosing a representative for ϕ , ϕ_τ , we have a piecewise linear function single-valued on $\Delta_{(S,D)}/\tau$ and one can consider the graph $\Gamma(\Delta_{(S,D)}/\tau, \phi_\tau)$. If τ lies as the one-cell separating two two-cells, σ_+ and σ_- , let ϕ_{σ_\pm} be the linear extensions of ϕ_τ restricted to the maximal cones σ_\pm . Then we have canonical inclusions of graphs and an equality

$$(4.1) \quad \Gamma(\Delta_{(S,D)}/\tau, \phi_\tau) = \Gamma(\Delta_{(S,D)}/\sigma_+, \phi_{\sigma_+}) \cap \Gamma(\Delta_{(S,D)}/\sigma_-, \phi_{\sigma_-}).$$

All the monoids $\Gamma(\Delta_{(S,D)}/\rho, \phi_\rho)$ have actions by M , giving rings

$$k[\Gamma(\Delta_{(S,D)}/\rho), \phi_\rho]$$

with $k[M]$ -algebra structures, and different choices of representative for ϕ lead to canonically isomorphic $k[M]$ -algebras. Choose a monomial ideal $I \subset M$ such

that $A_I := k[M]/I$ is Artinian, and write

$$k[\Gamma(\Delta_{(S,D)}/\rho), \phi_\rho]_I := k[\Gamma(\Delta_{(S,D)}/\rho), \phi_\rho] \otimes_{k[M]} A_I.$$

Let

$$U_\rho = \text{Spec } k[\Gamma(\Delta_{(S,D)}/\rho), \phi_\rho]_I.$$

Then the relation (4.1) leads to natural open inclusions $U_{\sigma_\pm} \subset U_\tau$, which gives us gluing data for a scheme. The paper [8] gives explicit formulae for the rings involved and proves that this gluing data does indeed satisfy the descent condition. This is the strict analogue of the Mumford degeneration, but does not contain any data about the instanton corrections. In particular, with the above gluing, it is not obvious that the glued scheme will carry enough global functions to be embedded into an affine variety. For example, a naive approach to finding global functions is to attempt to extend monomial functions from U_ρ , but this frequently doesn't work precisely because of monodromy. The authors of [8] correct the gluing using automorphisms of the rings $k[\Gamma(\Delta_{(S,D)}/\sigma, \phi_\sigma)]_I$ for the two-cells σ and taking a limit over all I .

Suppose that we have a scattering diagram $(f, \Delta_{(S,D)}, R, J)$ and fix a thickening ideal I . Let σ be a two-cell with boundary one-cells τ_+, τ_- . Choose points $P_+, P_- \in \sigma$ very close to τ_+, τ_- respectively. Choose a path γ connecting P_+ to P_- . Such a path selects a primitive normal vector $n_\mathfrak{d}$ to each ray through the origin in σ , pairing negatively with the tangent vector of the path. By assumption there are only finitely many rays \mathfrak{d} passing through the origin such that $f(\mathfrak{d})$ is not 1 mod I . To each such ray take $\theta_\mathfrak{d}$ to be the automorphism defined on a toric monomial $z^p, p \in \Gamma(\Delta_{(S,D)}/\sigma, \phi_\sigma)$ by

$$\theta_\mathfrak{d}(z^p) = z^p f(\mathfrak{d})^{\langle n_\mathfrak{d}, r(p) \rangle}.$$

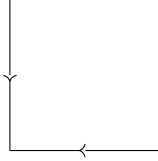
Now we define the automorphism θ_σ to be the ordered composition of the $\theta_\mathfrak{d}$ as one moves along γ . This yields an automorphism of U_σ . In addition, the definition of U_τ is modified slightly using $f(\tau)$, see [8], Equation (2.7). Thus we obtain a modification of the U_τ 's and a modification of the gluing inclusions $U_{\tau_+} \supset U_\sigma \subset U_{\tau_-}$. This gives a new glued scheme which depends on the scattering diagram and the ideal I . Consistent scattering diagrams then have the property that the associated rings have a natural basis of regular functions $\{\vartheta_p \mid p \in \Delta_{(S,D)}(\mathbb{Z})\}$ which yield an embedding in an affine scheme over $\text{Spec } A_I$. One of the main theorems of [8], namely Theorem 3.8, states the canonical scattering diagram is consistent. Importantly there is an algorithmic way of computing consistent scattering diagrams in certain situations, and a way of reducing the calculation of the canonical scattering diagram to these situations.

So for the moment, consider a case where $\Delta_{(S,D)}$ is in fact affine isomorphic to \mathbb{R}^2 and ϕ is single-valued. Then the sheaf \mathcal{M}^+ extends across 0, with the stalk at 0 being $\Gamma(\Delta_{(S,D)}, \phi)$. In this construction \mathcal{R}_0 is the completion of $k[\mathcal{M}_0^+]$ at its maximal monomial ideal. All of the automorphisms θ_σ act on \mathcal{R}_0 . Our construction so far has not attempted to incorporate the monoid ring

\mathcal{R}_0 . Take a cyclic ordering of the two-cells $\sigma_1, \dots, \sigma_n$ and let θ be the composite $\theta_{\sigma_n} \circ \dots \circ \theta_{\sigma_1}$ considered as a map $\mathcal{R}_0 \rightarrow \mathcal{R}_0$. Then the scattering diagram is consistent if the map θ is the identity, see [4] and [8], Theorem 3.30. Let us give an example calculation.

Example 4.1. Any toric variety relative to its toric boundary has trivial canonical scattering diagram. Therefore we will find no interesting examples here. Let us give an example motivated instead by dP_5 : we will see shortly the connection.

Our initial scattering diagram is \mathbb{R}^2 with two incoming rays $(1 + z^{(1,0)})$ and $(1 + z^{(0,1)})$:



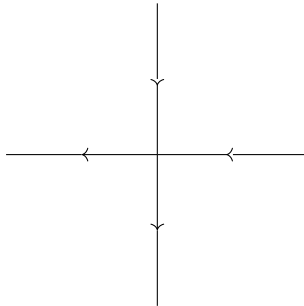
Let us calculate the composition θ along a circle anti-clockwise around the origin starting at $(-1, -2)$ acting on $z^{(1,0)}$ and $z^{(0,1)}$. The first wall we meet is $\mathfrak{d}_1 = \mathbb{R}_{\geq 0}(1, 0)$. Applying the above definition of the automorphism θ :

$$\begin{aligned} \theta_{\mathfrak{d}_1}(z^{(1,0)}) &= z^{(1,0)}(1 + z^{(1,0)})^{\langle(1,0),(0,-1)\rangle} = z^{(1,0)}, \\ \theta_{\mathfrak{d}_1}(z^{(0,1)}) &= z^{(0,1)}(1 + z^{(1,0)})^{\langle(0,1),(0,-1)\rangle} = z^{(0,1)}(1 + z^{(1,0)})^{-1}. \end{aligned}$$

Continuing along our path we meet the wall $\mathfrak{d}_2 = \mathbb{R}_{\geq 0}(0, 1)$. Here $\theta_{\mathfrak{d}_2}$ is given by:

$$\begin{aligned} \theta_{\mathfrak{d}_2}(z^{(1,0)}) &= z^{(1,0)}(1 + z^{(0,1)})^{\langle(1,0),(1,0)\rangle} = z^{(1,0)}(1 + z^{(0,1)}), \\ \theta_{\mathfrak{d}_2}(z^{(0,1)}) &= z^{(0,1)}(1 + z^{(0,1)})^{\langle(0,1),(1,0)\rangle} = z^{(0,1)}. \end{aligned}$$

Therefore the composition θ sends $z^{(1,0)}$ to $z^{(1,0)}(1 + z^{(0,1)})$ and $z^{(0,1)}$ to $z^{(0,1)}(1 + z^{(1,0)} + z^{(1,1)})^{-1}$. To first order this looks as if we are missing outgoing rays with monomials $(1 + z^{(1,0)})$ and $(1 + z^{(0,1)})$. Let us add those in and then repeat this calculation.



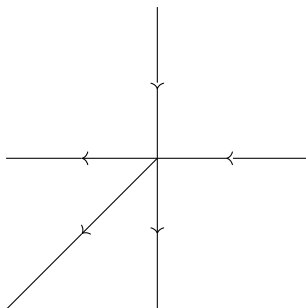
Taking again a path anti-clockwise starting at $(-1, -2)$ we first meet the wall $\mathfrak{d}_3 = \mathbb{R}_{\geq 0}(0, -1)$. The associated $\theta_{\mathfrak{d}_3}$ acts by:

$$\begin{aligned} \theta_{\mathfrak{d}_3}(z^{(1,0)}) &= z^{(1,0)}(1 + z^{(0,1)})^{\langle(1,0),(-1,0)\rangle} = z^{(1,0)}(1 + z^{(0,1)})^{-1}, \\ \theta_{\mathfrak{d}_3}(z^{(0,1)}) &= z^{(0,1)}(1 + z^{(0,1)})^{\langle(0,1),(-1,0)\rangle} = z^{(0,1)}. \end{aligned}$$

The next wall is \mathfrak{d}_1 , which again acts as before. The third wall we meet is \mathfrak{d}_2 , again acting as before. The final wall we encounter is $\mathfrak{d}_4 = \mathbb{R}_{\geq 0}(-1, 0)$, where the associated θ is given by:

$$\begin{aligned} \theta_{\mathfrak{d}_4}(z^{(1,0)}) &= z^{(1,0)}(1 + z^{(1,0)})^{\langle(1,0),(0,1)\rangle} = z^{(1,0)}, \\ \theta_{\mathfrak{d}_4}(z^{(0,1)}) &= z^{(0,1)}(1 + z^{(1,0)})^{\langle(0,1),(0,1)\rangle} = z^{(0,1)}(1 + z^{(1,0)}). \end{aligned}$$

One easily calculates the composite of all of these and one finds that to second order the composite acts by $z^{(1,0)} \mapsto z^{(1,0)}(1 + z^{(1,1)} + \dots)$ so it appears that we are missing an outgoing ray carrying monomial $(1 + z^{(1,1)})$. Introducing such a ray to obtain a new scattering diagram:



Now one calculates θ is the identity, so we have finally constructed a consistent scattering diagram.

The term-by-term nature of the above construction seems to suggest that in the background lurks a general procedure. The Kontsevich-Soibelman lemma of [13] proves that from any scattering diagram embedded in \mathbb{R}^2 (i.e., one with no singularities at the origin) one can construct a consistent scattering diagram by adding in only outgoing rays. In particular one can perform this correction order-by-order as in our example making it computable. This is explicitly described in the following lemma.

Lemma 4.2 (The Kontsevich-Soibelman lemma). *Let (B, f, R, J) be a scattering diagram with $B \cong \mathbb{R}^2$ as affine manifolds. Let P be a point of B contained inside a two-cell σ . The ordered composite of the functions θ along a path γ around the origin with $\gamma(0) = \gamma(1) = P$ gives rise to an automorphism θ_γ of the stalk of sheaf \mathcal{R} at zero. There exists another scattering diagram (B, f', R, J) such that the corresponding automorphism θ_γ is the identity and such that for each ray \mathfrak{d} one has*

$$f'(\mathfrak{d}) = f(\mathfrak{d})(1 + \sum a_i z^{m_i}),$$

where the z^{m_i} are all outgoing.

A key result of Gross, Hacking and Keel, Theorem 3.25 of [8] explores how to flatten the base of the scattering diagram by using *toric models*. A toric model of (S, D) is a choice of birational morphism $\phi : (S, D) \rightarrow (S', D')$ obtained by blowing down curves in the interior of S meeting D in precisely one point such that S' is toric and D' the toric boundary. This restricts to an isomorphism $D \cong D'$ and so induces a map of dual complexes which “flattens” the singularities in the sense that the ensuing dual intersection complex is isomorphic to \mathbb{R}^2 as an affine manifold. In the philosophy of Gross Hacking and Keel it pushes the singularities out to infinity. We reincorporate the singularities by instead including them into the scattering diagram as rays carrying expressions $1 + z^{[E_i] + \phi(v_i)}$ where E_i is an exceptional curve meeting D_i and v_i is the primitive generator of the ray in $\Delta_{(S', D')}$ corresponding to D_i . We make this construction explicit in the example in the next section. There is a canonical morphism $\nu : \Delta_{(S, D)} \rightarrow \Delta_{(S', D)}$ and in Lemmas 3.27 and 3.28 of [8] the authors prove that this induces an isomorphism of sheaves $\mathcal{R}(S, D) \cong \mathcal{R}(S', D)$ together with a bijection of broken lines between $\Delta_{(S, D)}$ and $\Delta_{(S', D)}$. To be precise we have the following theorem of [8]:

Theorem 4.3. *Let (S, D) be a Looijenga pair with (S', D) a toric model. Then the complex $\Delta_{S', D}$ is isomorphic as an affine manifold to \mathbb{R}^2 . Let*

$$(\mathbb{R}^2, f_{S'}, \underline{M}, \underline{M} \setminus 0)$$

be the scattering diagram with values in $A_1(S)$ on $\Delta_{(S', D')}$ whose value along $\mathbb{R}_{\geq 0}v_i$ is the product of incoming rays $\prod_j (1 + z^{[E_{i,j}] + \phi(v_i)})$ and outgoing rays $\prod_j (1 + z^{-[E_{i,j}] + \phi(v_i)})^{-1}$ where the $E_{i,j}$ are the blown-down curves meeting D_i . Since this satisfies the assumptions of the Kontsevich-Soibelman lemma, we let $\bar{f}_{S'}$ be the associated consistent diagram.

Let \bar{f}_S be the canonical scattering diagram on $\Delta_{(S, D)}$. Locally $\Delta_{(S, D)}$ and $\Delta_{(S', D')}$ are isomorphic and we can evaluate $f_{S'}$, \bar{f}_S and $\bar{f}_{S'}$ on the same line \mathfrak{d} . Then one has an equality

$$\bar{f}_{S'}(\mathfrak{d}) = \bar{f}_S(\mathfrak{d})f_{S'}(\mathfrak{d}),$$

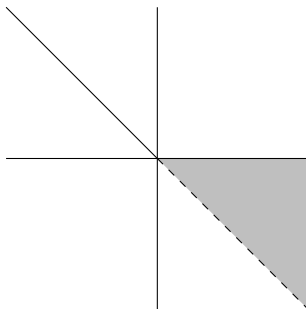
this has the effect of replacing the base of the scattering diagram by an affine manifold isomorphic to \mathbb{R}^2 and swapping the directions of rays $(1 + z^{[E_{i,j}] + \phi(v_i)})$ from outgoing to incoming. This is seen explicitly in the example in the next section.

After possibly blowing up some double points of D , we can then blow down appropriate curves to construct toric models, see [8], Proposition 1.3. This allows one to calculate the original scattering diagram by applying the Kontsevich-Soibelman lemma to $f_{S'}$. An implementation of this algorithm in Sage is available alongside this paper.

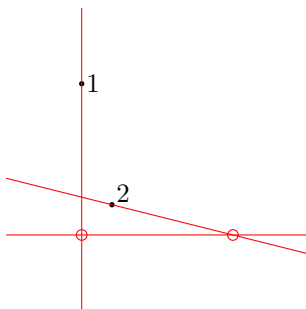
5. Explicit formulae

Let us practice constructing toric models in the cases we are interested in.

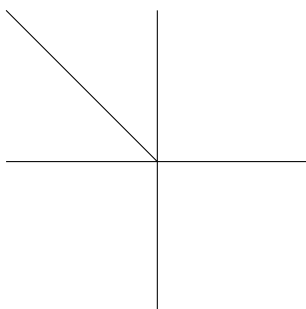
Example 5.1. Recall the dual intersection complex for dP_5 :



This is certainly not affine isomorphic to \mathbb{R}^2 . The boundary has five components, and this suggests that we should attempt to find a toric model isomorphic to dP_7 , since there is a choice of boundary divisor there also consisting of five components. A model for dP_7 together with its toric boundary is contained below. The red lines are a triangle in \mathbb{P}^2 , the red circles are blown up to obtain dP_7 , and the black points are further blown up to obtain dP_5 with dP_7 as its toric model.

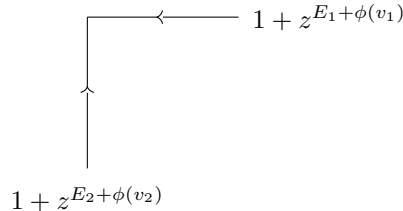


The corresponding dual complex is given by:

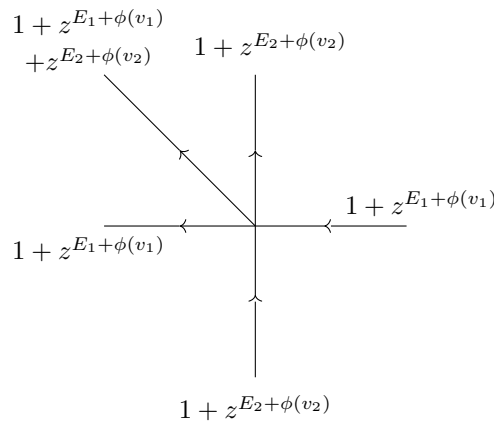


In particular the self intersection of every component of the boundary for dP_5 was -1 , whereas two of the components of the boundary of dP_7 have self intersection 0 .

We now incorporate this into the construction of the scattering diagram. Initially after making a choice of ordering we have the scattering diagram:



and we saw in our motivation for the Kontsevich-Soibelman lemma that this produces a consistent diagram:



which agrees up to changing the direction of the incoming rays and pushing forwards with the scattering diagram found in [8] Figure 1.1. This is exactly as predicted by the Kontsevich-Soibelman Lemma.

The attached implementation is optimised in three ways. Firstly one only is interested in terms of order n , so we may reduce all the series modulo terms of higher order and use efficient power calculations to do so. Secondly this can be distributed over multiple cores. Thirdly each ray stores a list of all powers already calculated so as to minimise repeat calculations. I would appreciate any input on how to significantly speed up this algorithm.

Since by the previous section only a finite collection of classes need be calculated we may terminate the calculation once those coefficients have been obtained and substitute them into the formulae (3.6)-(3.11) we found using the techniques in Section 2.2.2.

Recall that the Picard group of dP_d is generated by a hyperplane class H and the class of the exceptional curves E_1, \dots, E_{9-d} . By using the attached implementation of the Kontsevich-Soibelman lemma one can read off the desired coefficients and the resulting families are contained in Table 5.1.

TABLE 5.1. Explicit equations for mirror families

Surface	Equations	Super-potential
dP_5	$\vartheta_1\vartheta_3 = z^{[D_2]}\vartheta_2 + z^{[D_4]+[D_5]}$ $\vartheta_2\vartheta_4 = z^{[D_3]}\vartheta_3 + z^{[D_1]+[D_4]}$ $\vartheta_3\vartheta_5 = z^{[D_4]}\vartheta_4 + z^{[D_1]+[D_2]}$ $\vartheta_4\vartheta_1 = z^{[D_5]}\vartheta_5 + z^{[D_2]+[D_3]}$ $\vartheta_5\vartheta_2 = z^{[D_1]}\vartheta_1 + z^{[D_3]+[D_4]}$	$\sum \vartheta_i$
dP_4	$\vartheta_1\vartheta_3 = z^{[D_2]}\vartheta_2 + z^{[D_4]}\vartheta_4 +$ $z^{H-E_1} + z^{2H-E_1-E_2-E_3-E_5} + z^{2H-E_1-E_2-E_4-E_5}$ $\vartheta_2\vartheta_4 = z^{[D_1]}\vartheta_1 + z^{[D_3]}\vartheta_3 +$ $z^{H-E_3} + z^{H-E_4} + z^{2H-E_2-E_3-E_4-E_5}$	$\sum \vartheta_i$
dP_3	$\vartheta_1\vartheta_2\vartheta_3 = z^{[D_1]}\vartheta_1^2 + z^{[D_2]}\vartheta_2^2 + z^{[D_3]}\vartheta_3^2 +$ $z^{[D_1]}\vartheta_1(z^{E_1} + z^{E_2} + z^{H-E_3-E_5} + z^{H-E_3-E_6} +$ $z^{H-E_4-E_5} + z^{H-E_4-E_6}) + z^{[D_2]}\vartheta_2(z^{E_3} + z^{E_4} +$ $z^{H-E_1-E_5} + z^{H-E_1-E_6} + z^{H-E_2-E_5} + z^{H-E_2-E_6}) +$ $z^{[D_3]}\vartheta_3(z^{E_5} + z^{E_6} + z^{H-E_1-E_3} + z^{H-E_1-E_4}$ $z^{H-E_2-E_3} + z^{H-E_2-E_4}) + z^H +$ $(z^{2H} + z^{4H-\sum E_i})\alpha +$ $z^{3H-\sum E_i}(z^{E_2-E_1} + z^{E_1-E_2} + z^{E_4-E_3} + z^{E_3-E_4} +$ $z^{E_6-E_5} + z^{E_6-E_5}) + z^{5H-2\sum E_i} + 4z^{[D]}$ $\alpha = (z^{-E_1} + z^{-E_2})(z^{-E_3} + z^{-E_4})(z^{-E_5} + z^{-E_6})$	$\sum \vartheta_i$

The expression for the mirror family to dP_3 agrees with that found in [8], Example 6.13. To express the formulae for dP_2 requires some additional notation. In this case we had to blow up two additional points which lay on the intersection of the chosen conic C and line L . Let E_8, E_9 be the exceptional divisors lying over the intersections points of C and L . Let us relabel the ϑ_i by the cohomology class of the corresponding boundary divisor, e.g., writing ϑ_{D_i} for ϑ_i . There is an action of C_2 exchanging E_1 and E_2 , an action of S_5 permuting E_3 through E_7 and an action of C_2 exchanging E_8 and E_9 . When we write $\prod(1 + z^{hH + \sum a_i E_i})$ we mean to take the product of $1 + z^{h[H] + \sum a_i [E_i]}$ over elements of the orbit under the action of $C_2 \times S_5$. In particular we choose here representatives with $a_1 \geq a_2$ and a_3 through a_7 decreasing. For instance $\prod(1 + z^{H+E_3})$ would be the product $(1 + z^{H+E_3})(1 + z^{H+E_4})(1 + z^{H+E_5})(1 + z^{H+E_6})(1 + z^{H+E_7})$. Searching through

the output of our implementation of the Kontsevich-Soibelman lemma we are able to find the coefficients we were missing in the equations (3.6) to (3.11) for the mirror family to dP_2 relative to our choice of boundary. After calculating these we find that the mirror family is given by

$$\begin{aligned}
\vartheta_C \vartheta_L &= z^{E_8} \vartheta_{E_8} + z^{E_9} \vartheta_{E_9} + 3z^{C+L+2E_8+2E_9} + B_1(E_8)z^{E_8}, \\
\vartheta_{E_8} \vartheta_{E_9} &= \vartheta_{3L} z^L + \vartheta_{2L} B_1(L)z^L + \vartheta_L B_2(L)z^L \\
&\quad + z^C B_3(C) + 3z^{2C+2L+3E_8+3E_9} + \vartheta_C B_2(C)z^C \\
&\quad + \vartheta_{2C} B_1(C)z^C + \vartheta_{3C} z^C, \\
\vartheta_C^3 &= \vartheta_{3C} + 3B_1(L)z^{L+E_8+E_9} \vartheta_C + 6z^{C+2L+3E_8+3E_9} + 6B_1(E_9) \\
&\quad z^{L+E_8+2E_9} + 3z^{L+2E_8+E_9} \vartheta_{E_8} + 3z^{L+E_8+2E_9} \vartheta_{E_9}, \\
\vartheta_L^3 &= \vartheta_{3L} + 3B_1(C)z^{C+E_8+E_9} \vartheta_L + 6z^{2C+L+3E_8+3E_9} + 6B_1(E_8) \\
&\quad z^{C+2E_8+E_9} + 3z^{C+E_8+2E_9} \vartheta_{E_9} + 3z^{C+2E_8+E_9} \vartheta_{E_8}, \\
\vartheta_C^2 &= \vartheta_{2C} + 2\vartheta_L z^{L+E_8+E_9} + 2B_1(L)z^{L+E_8+E_9}, \\
\vartheta_L^2 &= \vartheta_{2L} + 2\vartheta_C z^{C+E_8+E_9} + 2B_1(C)z^{C+E_8+E_9},
\end{aligned}$$

where the coefficients $B_k(E)$ are terms in the scattering diagram related to the relative invariants of curves meeting the curve E in one point with tangency order k . The term $B_i(-)$ is the coefficient of t^i in the product $\prod N_k(-, t^k)$, where the $N_k(-, t)$ are given by the following formulae:

$$\begin{aligned}
N_3(C, t) &= \prod (1 + 9tz^{2H-E_1-E_2-E_3}) \prod (1 + 9tz^{3H-2E_1-E_2-E_3-E_4-E_5}) \\
&\quad \prod (1 + 9tz^{4H-2E_1-2E_2-2E_3-E_4-E_5-E_6}) \\
&\quad \prod (1 + 9tz^{4H-3E_1-E_2-E_3-E_4-E_5-E_6-E_7}) \\
&\quad \prod (1 + 72tz^{4H-2E_1-2E_2-E_3-E_4-E_5-E_6-E_7}) \\
&\quad \prod (1 + 9tz^{5H-3E_1-2E_2-2E_3-2E_4-E_5-E_6-E_7}) \\
&\quad \prod (1 + 9tz^{6H-3E_1-3E_2-2E_3-2E_4-2E_5-2E_6-E_7}), \\
N_2(C, t) &= \prod (1 + 4tz^{H-E_1}) \prod (1 + 4tz^{2H-E_1-E_2-E_3-E_4}) \\
&\quad \prod (1 + 4tz^{3H-2E_1-E_2-E_3-E_4-E_5-E_6}) \\
&\quad \prod (1 + 4tz^{4H-2E_1-2E_2-2E_3-E_4-E_5-E_6-E_7}), \\
N_1(C, t) &= \prod (1 + tz^{E_3}) \prod (1 + tz^{H-E_1-E_3}) \\
&\quad \prod (1 + tz^{2H-E_1-E_2-E_3-E_4-E_5}) \\
&\quad \prod (1 + tz^{3H-2E_1-2E_2-2E_3-E_4-E_5-E_6})
\end{aligned}$$

$$\begin{aligned}
N_3(L, t) &= \prod (1 + 9tz^{3H-2E_3-E_4-E_5-E_6-E_7}) \\
&\prod (1 + 9tz^{4H-E_1-2E_3-2E_4-2E_5-E_6-E_7}) \\
&\prod (1 + 9tz^{5H-E_1-E_2-3E_3-2E_4-2E_5-2E_6-E_7}) \\
&\prod (1 + 72tz^{5H-E_1-E_2-2E_3-2E_4-2E_5-2E_6-2E_7}) \\
&\prod (1 + 9tz^{5H-2E_1-2E_3-2E_4-2E_5-2E_6-2E_7}) \\
&\prod (1 + 9tz^{6H-2E_1-E_2-3E_3-3E_4-2E_5-2E_6-2E_7}) \\
&\prod (1 + 9tz^{7H-2E_1-2E_2-3E_3-3E_4-3E_5-3E_6-2E_7}), \\
N_2(L, t) &= \prod (1 + 4tz^{2H-E_3-E_4-E_5-E_6}) \\
&\prod (1 + 4tz^{3H-E_1-2E_3-E_4-E_5-E_6-E_7}) \\
&\prod (1 + 4tz^{4H-E_1-E_2-2E_3-2E_4-2E_5-E_6-E_7}) \\
&\prod (1 + 4tz^{5H-2E_1-E_2-2E_3-2E_4-2E_5-2E_6-2E_7}), \\
N_1(L, t) &= \prod (1 + tz^{E_1}) \prod (1 + tz^{H-E_3-E_4}) \\
&\prod (1 + tz^{2H-E_1-E_3-E_4-E_5-E_6}) \\
&\prod (1 + tz^{3H-E_1-E_2-2E_3-E_4-E_5-E_6-E_7}), \\
N_1(E_8, t) &= \prod (1 + tz^{H-E_3-E_8}) \prod (1 + tz^{2H-E_1-E_3-E_4-E_5-E_8}) \\
&\prod (1 + 9tz^{3H-E_1-E_2-E_3-E_4-E_5-E_6-E_7-E_8}) \\
&\prod (1 + tz^{3H-E_1-E_2-2E_3-E_4-E_5-E_6-E_8}) \\
&\prod (1 + tz^{3H-2E_1-E_3-E_4-E_5-E_6-E_7-E_8}) \\
&\prod (1 + tz^{4H-2E_1-E_2-2E_3-2E_4-E_5-E_6-E_7-E_8}) \\
&\prod (1 + tz^{5H-2E_1-2E_2-2E_3-2E_4-2E_5-2E_6-E_7-E_8}), \\
N_1(E_9, t) &= \prod (1 + tz^{H-E_3-E_9}) \prod (1 + tz^{2H-E_1-E_3-E_4-E_5-E_9}) \\
&\prod (1 + 9tz^{3H-E_1-E_2-E_3-E_4-E_5-E_6-E_7-E_9}) \\
&\prod (1 + tz^{3H-E_1-E_2-2E_3-E_4-E_5-E_6-E_9}) \\
&\prod (1 + tz^{3H-2E_1-E_3-E_4-E_5-E_6-E_7-E_9}) \\
&\prod (1 + tz^{4H-2E_1-E_2-2E_3-2E_4-E_5-E_6-E_7-E_9}) \\
&\prod (1 + tz^{5H-2E_1-2E_2-2E_3-2E_4-2E_5-2E_6-E_7-E_9}).
\end{aligned}$$

After setting all of the monomials equal to one we find that the values of $B_i(-)$ reduce to 6561, 459, 27, 6561, 459, 27, 81 and 81 respectively and this fibre of the family is smooth. We will use this model for calculations later. We expect that each fibre of this family is a double cover of the plane. This can be seen by projecting onto ϑ_C and ϑ_L , then the equations are entirely symmetric under exchanging these two variables, noting that $z^C B_3(C) = z^L B_3(L)$.

Unfortunately this is a deformation of the four-vertex, not of the two-vertex. This stems from our decision to blow up two additional points at the start, and so the family we actually want is the restriction to the locus $z^{E_8} = z^{E_9} = 1$. Setting $z^C = z^L = 0$ we see that coordinates on the central fibre are ϑ_C, ϑ_L and $\vartheta_{E_8} - \vartheta_{E_9}$. Eliminating the extra variables we obtain an equation for the family:

Theorem 5.2. *Let S be a degree two del Pezzo surface and D an anti-canonical cycle of rational curves. Then the mirror family is explicitly a hyperplane in $\mathbb{A}^3 = \text{Spec } k[\vartheta_C, \vartheta_L, \vartheta_{E_8} - \vartheta_{E_9}]$ defined by the equation:*

$$\begin{aligned}
 (\vartheta_{E_8} - \vartheta_{E_9})^2 = & \vartheta_C^2 \vartheta_L^2 - 4\vartheta_C^3 z^C - 4\vartheta_L^3 z^L + 18\vartheta_C \vartheta_L z^{C+L} - 27z^{2C+2L} \\
 & - 4\vartheta_L^2 z^L B_1(L) - 4\vartheta_C^2 z^C B_1(C) + 20\vartheta_C z^{C+L} B_1(L) \\
 & + 20\vartheta_L z^{C+L} B_1(C) + 16z^{C+L} B_1(L) B_1(C) - 4\vartheta_L z^L B_2(L) \\
 & - 4\vartheta_C z^C B_2(C) - 2\vartheta_C \vartheta_L B_1(E_8) + 30z^{C+L} B_1(E_8) \\
 (5.1) \quad & - 4z^C B_3(C) - B_1(E_8)^2.
 \end{aligned}$$

It is a double cover of \mathbb{A}^2 branching over a quartic curve.

Now we see clearly the leading order terms $\vartheta_C^2 \vartheta_L^2 = (\vartheta_{E_8} - \vartheta_{E_9})^2$, giving rise to the two-vertex over the origin. The appropriate super-potential remains $\vartheta_C + \vartheta_L$.

One could ask if there is a better way to present the data hiding in the scattering diagram. In the cases of dP_5 and dP_4 the canonical scattering diagram is finite and can be computed, as was done in Example 3.7 of [8] for one of these. By an observation of Gross, Hacking and Keel the entire scattering diagram for dP_3 is generated by the series associated to a single ray under the birational automorphism group of this surface, generated by a finite collection of classes. This breaks down in lower degrees, as far as I am aware there is no known closed form expression for the scattering diagram associated to the final surface.

There are however more elegant ways to describe terms arising in the equation, as was seen in Example 6.13 of [8]. Following these ideas we can describe the terms arising in equation 5.1. To do this we write $N_i(-, t)^{(j)}$ for the coefficient of t^j in $N_i(-, t)$. Then we find the following birational descriptions:

Term	Description
$N_1(C, t)^{(1)} z^C$	The sum of $\frac{1}{16} z^{\pi^*(H-E)}$ over all contractions to dP_8 obtained by contracting one -1 -curve meeting C and five meeting L , none of which meet π^*E or π^*H .
$N_1(L, t)^{(1)} z^L$	The sum of $\frac{1}{16} z^{\pi^*(H-E)}$ over all contractions to dP_8 obtained by contracting one -1 -curve meeting L and five meeting C , none of which meet π^*E or π^*H .
$N_1(C, t)^{(2)} z^C$	The sum of z^{π^*H} over all contractions to \mathbb{P}^2 obtained by blowing down two -1 -curves meeting C and five meeting L .
$N_1(L, t)^{(2)} z^L$	The sum of z^{π^*H} over all contractions to \mathbb{P}^2 obtained by blowing down two -1 -curves meeting L and five meeting C .
$N_2(C, t)^{(1)} z^C$	The sum of $4z^{\pi^*K_S}$ over all contractions of a single -1 -curve meeting L and not meeting C .
$N_2(L, t)^{(1)} z^C$	The sum of $4z^{\pi^*K_S}$ over all contractions of a single -1 -curve meeting C and not meeting L .
$N_1(E_8, t)^{(1)} z^{E_8}$	The sum of $z^{\pi^*(H-E)}$ over all contractions to dP_8 obtained by contracting four -1 -curves meeting one of C or L and three meeting the other.

The term $\frac{1}{16}$ in $N_1(C, t)^{(1)} z^C$ arises because given one of these classes α there are sixteen -1 -curves (each of degree at most three) meeting α and C but not meeting L . Fixing any one of these produces a unique contraction contributing to the desired monomial. In other words a subgroup of the birational automorphism group of the surface stabilises the class α . Finally we observe by direct computation that $z^C N_3(C, t)^{(1)} = 9z^{C+L} N_1(E_8, t)^{(1)} - 9z^{-2K_S}$. This gives a birational interpretation of every term appearing in equation 5.1.

6. Evidence for the construction

We begin this section by comparing the predictions of [3] for the mirror families. These predictions state the mirror to dP_n ought to be a compactification of a fibration of the two-torus $W : \mathbb{G}_m^2 \rightarrow \mathbb{C}$ with an I_n fibre at infinity. Here W is the super-potential. For example, in the case of dP_5 we can take equations:

$$x_{i+1}x_{i-1} = x_i + 1$$

defining a surface inside \mathbb{A}^5 with $W = \sum x_i$. It turns out this is already a partial compactification of the mirror to dP_5 . To further compactify, we take the projective closure of the above surface, taking coordinates Z_1, \dots, Z_5 and T to obtain equations

$$Z_{i+1}Z_{i-1} = Z_iT + T^2.$$

Then T, W can be viewed as sections of $\mathcal{O}(1)$ on this surface, hence giving a pencil. After resolving the base-points of this pencil, one obtains the desired compactification. The fibre at infinity therefore has equations

$$Z_{i-1}Z_{i+1} = 0$$

for $i \in \{1, 2, 3, 4, 5\}$ inside \mathbb{P}^4 , hence defining a cycle of five planes. This is exactly as predicted by [3]. For the other del Pezzo surfaces dP_n with $n \geq 4$, the same shape of the mirror as defined by quadratic equations confirms that the fibre at infinity will be an I_n fibre. More careful considerations with the equations show the same for $n = 3$ and 2.

We can also check that the Jacobian ring is the correct rank. Conjecturally the quantum cohomology of S is isomorphic to the Jacobian ring of (\check{V}, \check{W}) .

If S is a del Pezzo surface of degree d then the rank of the middle homology is $10 - d$, generated by a hyperplane and the exceptional curves. Therefore the rank of the quantum cohomology should be $12 - d$. Now let (\check{V}, \check{W}) be a smooth fibre of the family such that \check{W} has isolated critical points. The rank of the Jacobian ring of \check{W} should then be equal to $12 - d$.

Let us attempt this calculation for the case of the mirror to dP_2 . First recall that the super-potential on LG model is the partial sum $x_C + x_L$.

Example 6.1. The Jacobian ring of $(S, W : S \rightarrow \mathbb{C})$ is the function ring of the critical points of W . In our case S is defined by two equations in \mathbb{A}^4 , f_1 and f_2 . Therefore we are interested in the points of S where ∇W is contained in the span of ∇f_1 and ∇f_2 . This asks that all the 3×3 minors of the following matrix vanish

$$M = \begin{bmatrix} \partial f_1 / \partial \vartheta_C & \partial f_1 / \partial \vartheta_L & \partial f_1 / \partial \vartheta_8 & \partial f_1 / \partial \vartheta_9 \\ \partial f_2 / \partial \vartheta_C & \partial f_2 / \partial \vartheta_L & \partial f_2 / \partial \vartheta_8 & \partial f_2 / \partial \vartheta_9 \\ \partial W / \partial \vartheta_C & \partial W / \partial \vartheta_L & \partial W / \partial \vartheta_8 & \partial W / \partial \vartheta_9 \end{bmatrix}.$$

This can be calculated using Sage and setting all the coefficients to one we find that generating elements of the defining ideal are:

$$(6.1) \quad \begin{aligned} &(\vartheta_9 + 2)\vartheta_C + 3\vartheta_C^2 - (\vartheta_9 + 2)\vartheta_L - 3\vartheta_L^2 + 58\vartheta_C - 58\vartheta_L, \\ &(\vartheta_8 + 2)\vartheta_C + 3\vartheta_C^2 - (\vartheta_8 + 2)\vartheta_L - 3\vartheta_L^2 + 58\vartheta_C - 58\vartheta_L, \\ &-\vartheta_8 + \vartheta_9, -\vartheta_8 + \vartheta_9, \vartheta_C\vartheta_L - \vartheta_8 - \vartheta_9 - 84, \\ &-\vartheta_C^3 - \vartheta_L^3 + \vartheta_8\vartheta_9 - 27\vartheta_C^2 + 4\vartheta_C\vartheta_L - 27\vartheta_L^2 + 2\vartheta_8 + 2\vartheta_9 \\ &- 324\vartheta_C - 324\vartheta_L - 3000. \end{aligned}$$

Sage allows us to calculate a k -basis of the quotient ring and we find that the quotient is 10-dimensional as a vector space, exactly as expected.

References

- [1] N. H. Argz, *Log geometric techniques for open invariants in mirror symmetry*, PhD thesis, University of Hamburg, 2016.
- [2] D. Auroux, *Mirror symmetry and T-duality in the complement of an anticanonical divisor*, J. Gökova Geom. Topol. GGT **1** (2007), 51–91.
- [3] D. Auroux, L. Katzarkov, and D. Orlov, *Mirror symmetry for del Pezzo surfaces: vanishing cycles and coherent sheaves*, Invent. Math. **166** (2006), no. 3, 537–582. <https://doi.org/10.1007/s00222-006-0003-4>
- [4] M. Carl, M. Pumperla, and B. Siebert, *A tropical view of Landau-Ginzburg models*, 04, 2018.
- [5] M. W. Cheung, M. Gross, G. Muller, G. Musiker, D. Rupel, S. Stella, and H. Williams, *The greedy basis equals the theta basis: a rank two haiku*, J. Combin. Theory Ser. A **145** (2017), 150–171. <https://doi.org/10.1016/j.jcta.2016.08.004>
- [6] C.-H. Cho and Y.-G. Oh, *Floer cohomology and disc instantons of Lagrangian torus fibers in Fano toric manifolds*, Asian J. Math. **10** (2006), no. 4, 773–814. <https://doi.org/10.4310/AJM.2006.v10.n4.a10>
- [7] D. A. Cox, J. B. Little, and H. K. Schenck, *Toric Varieties*, Graduate Studies in Mathematics, **124**, American Mathematical Society, Providence, RI, 2011. <https://doi.org/10.1090/gsm/124>

- [8] M. Gross, P. Hacking, and S. Keel, *Mirror symmetry for log Calabi-Yau surfaces I*, Publ. Math. Inst. Hautes Études Sci. **122** (2015), 65–168. <https://doi.org/10.1007/s10240-015-0073-1>
- [9] M. Gross, P. Hacking, S. Keel, and M. Kontsevich, *Canonical bases for cluster algebras*, J. Amer. Math. Soc. **31** (2018), no. 2, 497–608. <https://doi.org/10.1090/jams/890>
- [10] M. Gross, P. Hacking, and B. Siebert, *Theta functions on varieties with effective anticanonical class*, ArXiv e-prints, January 2016.
- [11] M. Gross and B. Siebert, *Logarithmic Gromov-Witten invariants*, J. Amer. Math. Soc. **26** (2013), no. 2, 451–510. <https://doi.org/10.1090/S0894-0347-2012-00757-7>
- [12] ———, *Theta functions and mirror symmetry*, in Surveys in differential geometry 2016. Advances in geometry and mathematical physics, 95–138, Surv. Differ. Geom., **21**, Int. Press, Somerville, MA, 2016.
- [13] M. Kontsevich and Y. Soibelman, *Affine structures and non-Archimedean analytic spaces*, in The unity of mathematics, 321–385, Progr. Math., **244**, Birkhäuser Boston, Boston, MA, 2006. https://doi.org/10.1007/0-8176-4467-9_9
- [14] E. Looijenga, *Rational surfaces with an anticanonical cycle*, Ann. of Math. (2) **114** (1981), no. 2, 267–322. <https://doi.org/10.2307/1971295>
- [15] G. Mikhalkin, *Amoebas of algebraic varieties and tropical geometry*, in Different faces of geometry, 257–300, Int. Math. Ser. (N. Y.), **3**, Kluwer/Plenum, New York, 2004. https://doi.org/10.1007/0-306-48658-X_6
- [16] D. Mumford, *An analytic construction of degenerating abelian varieties over complete rings*, Compositio Math. **24** (1972), 239–272.

LAWRENCE JACK BARROTT
NATIONAL CENTER FOR THEORETICAL SCIENCES
NO. 1 SEC. 4 ROOSEVELT RD., NATIONAL TAIWAN UNIVERSITY
TAIPEI, 106, TAIWAN
Email address: lawrencebarrott@gmail.com